ICME 2026

Contact me by xuhaonan.site

TEAR of the SUNSET: A Benchmark for Road Detection in Off-Road Environment

Haonan Xu[1,2], Qirui Hu[1,2], Xinyuan Liu[1,2], Hu Li[1,2], Hang Xu[3], Yike Ma[†1], Yucheng Zhang[1], Feng Dai[1]

[1]Institute of Computing Technology, Chinese Academy of Sciences [2]University of Chinese Academy of Sciences [3]Hangzhou Dianzi University [†]Corresponding Author

1. Motivation

(a) and (b) demonstrate significant geometric differences in road morphologies between structured environments and semi-structured environments. For the former, lane markings strictly adhere to a single valued correspondence in the Cartesian coordinate. For the latter, road edge lines with large curvatures exhibit multi-valued correspondences. (c) presents the logarithmic curvature distribution at each line sampling point for traffic environments (CULane and TuSimple) and semi-structured environments (SUNSET) in the form of a heatmap. Solid lines of different colors represent the curvature of each dataset at each sampling point.

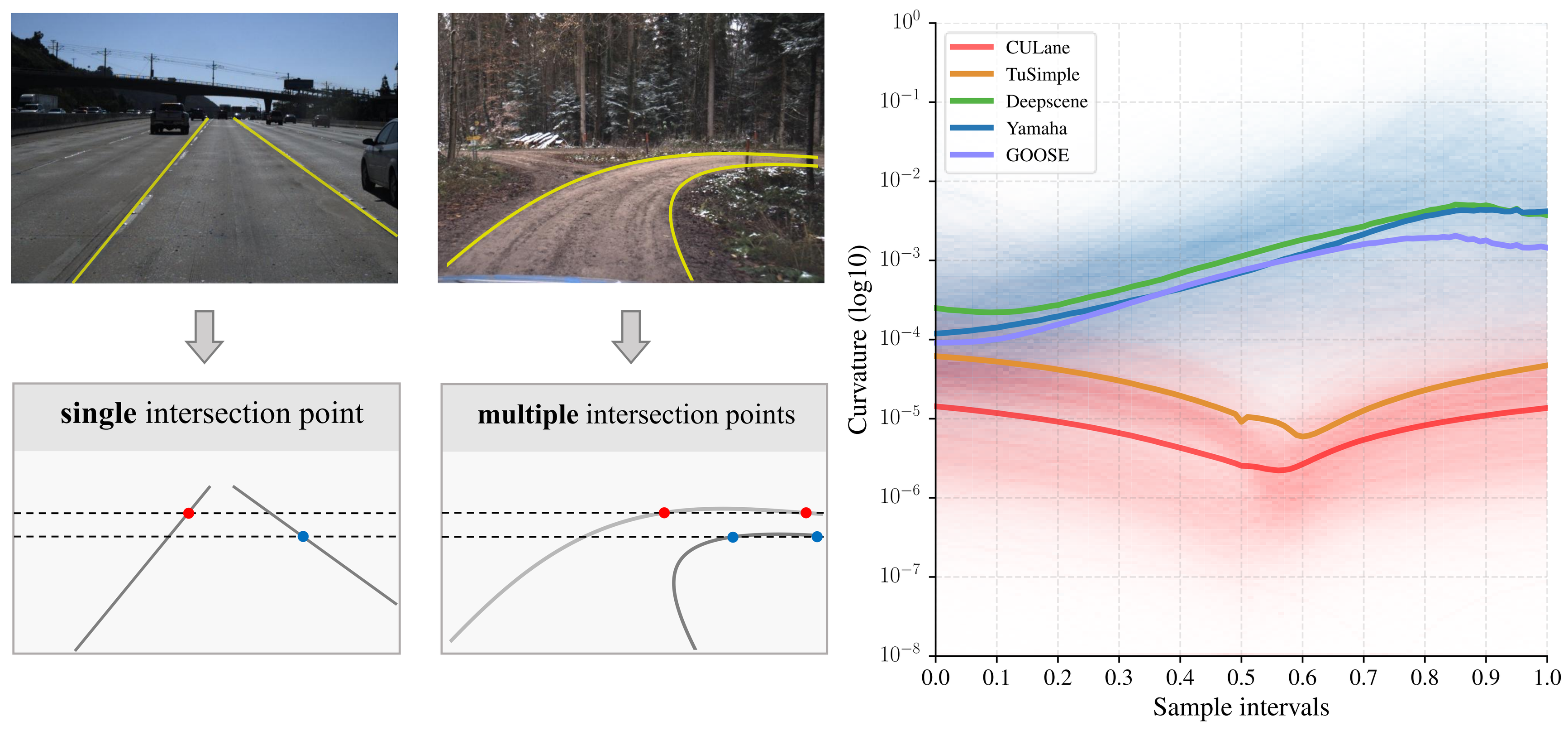

(a) (b) (c)

2. Methodology

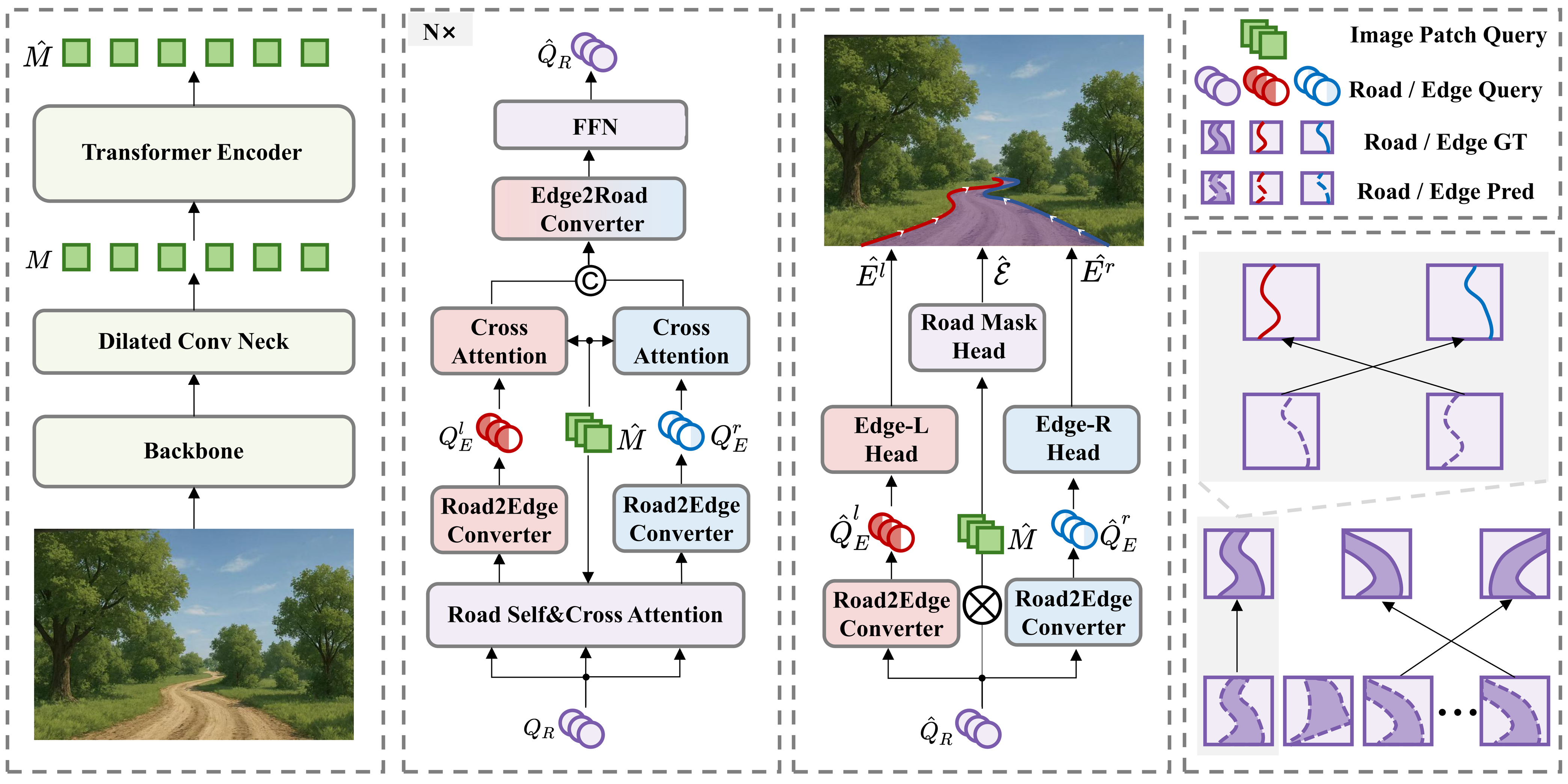

(a) Image Encoder (b) I-DI Decoder (c) Road-Edge Head

2.1 Task Definition

Line Instance: $E(t)=\sum_{i=0}^{n} b_{i,n}(t)\mathcal{P}_i, 0\le t\le 1, b_{i,n}=C_n^i t^i(1-t)^{n-i}, i=0,\dots,n$

Road Instance: $\Omega(u,t)=uE^l(t)+(1-u)E^r(t), t\in[0,1], u\in[0,1]$

2.2 Interconvertible Dual-Instance Decoder

$$Q_E^l=\mathcal{T}^{\,l}_{RE}(Q_R);\quad Q_E^r=\mathcal{T}^{\,r}_{RE}(Q_R)\quad \mid \quad \bar{Q}_R=\mathcal{T}_{ER}(\mathrm{Concat}(Q_E^l,Q_E^r))$$

2.3 Hierarchical Bipartite Match

$$\hat{\sigma}_R=\underset{\sigma_R\in\mathfrak{S}_{N_R}}{\arg\min}\sum_{i=1}^{N_R}\mathcal{C}_{R\mathrm{match}}\left(z_i,\hat{z}_{\sigma_R(i)}\right)\qquad \mathfrak{S}_2^{(i)}=\begin{Bmatrix}\{\, y_1^{(i)}\Leftrightarrow \hat{y}_1^{\sigma_R(i)},\ y_2^{(i)}\Leftrightarrow \hat{y}_2^{\sigma_R(i)}\,\},\\ \{\, y_1^{(i)}\Leftrightarrow \hat{y}_2^{\sigma_R(i)},\ y_2^{(i)}\Leftrightarrow \hat{y}_1^{\sigma_R(i)}\,\}\end{Bmatrix}$$

$\mathbb{T}: \hat{z}_i \Leftrightarrow \{\hat{y}_1^{(i)},\hat{y}_2^{(i)}\}$

$$\hat{\pi}_E=\underset{\pi_E\in\mathfrak{S}_2}{\arg\min}\underbrace{\sum_{j=1}^{2}\mathcal{C}_{E\mathrm{match}}\left(y_j,\hat{y}_{\pi_E(j)}\right)}_{\mathcal{C}_{R\mathrm{match}}\left(z_i,\hat{z}_{\sigma_R(i)}\right)}$$

3. Experiments

3.1 Metrics

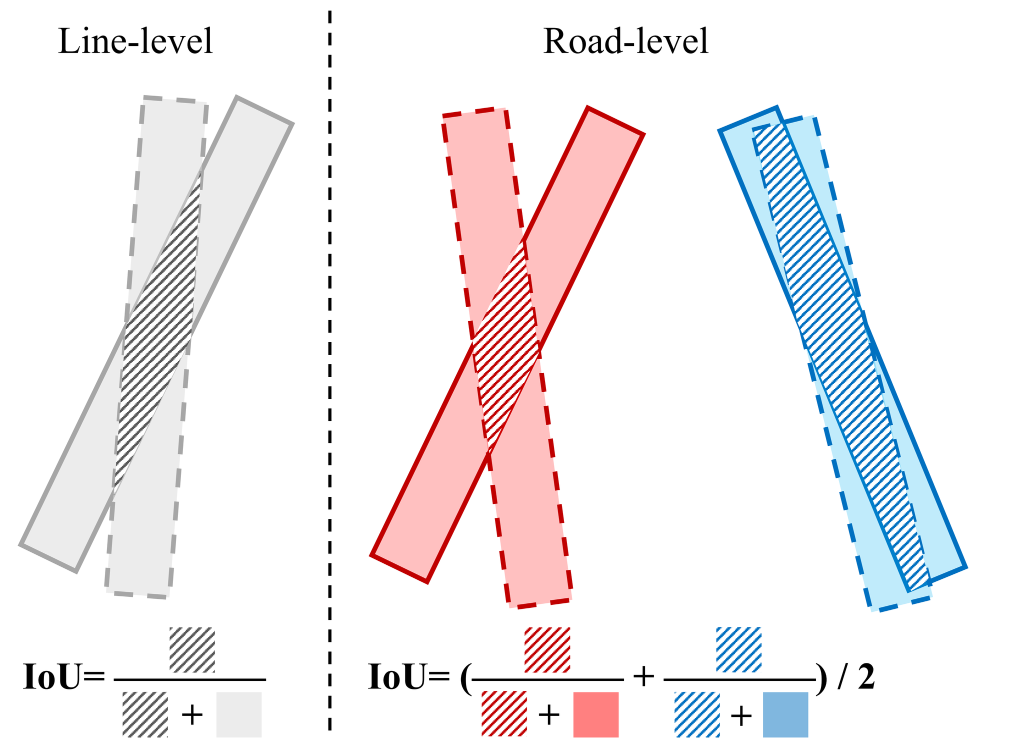

3.2 Main Results

	Methods	Publication	Backbone	DeepScene $F1_E$	DeepScene $F1_R$	YCOR $F1_E$	YCOR $F1_R$	GOOSE $F1_E$	GOOSE $F1_R$	SUNSET $F1_E$	SUNSET $F1_R$	Para(M)	FLOPs(G)
♠Segmentation	▼ ***Mask based***												
	SCNN [11]	*AAAI'18*	VGG16	52.26	-	31.75	-	30.67	-	43.72	-	23.73	183.54
	RESA [9]	*AAAI'21*	R-34	56.29	-	33.89	-	34.41	-	48.51	-	12.70	114.01
	▼ ***Keypoints based***												
	GANet [12]	*CVPR'22*	R-18	58.44	-	37.87	-	34.33	-	50.69	-	30.66	30.92
	CondLSTR [13]	*ICCV'23*	R-34	54.10	-	31.92	-	36.41	-	47.18	-	26.88	24.40
♣Detection	▼ ***Line-Anchor based***												
	SRLane [14]	*AAAI'24*	R-18	60.75	-	37.57	-	34.67	-	52.16	-	11.56	18.97
	LaneATT [15]	*CVPR'21*	R-18	51.31	-	38.48	-	32.51	-	45.57	-	23.01	42.73
	▼ ***Curve based***												
	BezierLaneNet [4]	*CVPR'22*	R-34	29.53	-	23.60	-	19.36	-	29.03	-	9.05	32.31
	LSTR [16]	*WACV'21*	R-18	48.15	-	31.07	-	30.52	-	40.56	-	21.94	38.18
	▼ ***Ours***												
	TEAR-S (ResNet18+E2/D2)	-	R-18	68.43	69.57	38.31	33.85	35.89	33.66	59.60	59.81	5.64	19.12
	TEAR-M (ResNet34+E3/D3)	-	R-34	**70.51**	73.07	**39.63**	40.29	**36.64**	34.74	**61.27**	62.56	11.88	38.09

3.3 Visualized Results